Cement & Concrete Composites **12** (1990) 233–244

Durability Studies and Characterization of the Matrix and Fibre–Cement Interface of Asbestos-Free Fibre–Cement Products

B. J. Pirie, F. P. Glasser

Department of Chemistry, University of Aberdeen, Meston Walk, Old Aberdeen, AB9 2UE, UK

C. Schmitt-Henco & S. A. S. Akers

Ametex AG, CH-8867 Niederurnen, Switzerland

(Received 10 February 1989; accepted 17 September 1990)

Abstract

Organic fibres, both natural and synthetic, have been used as asbestos replacements in cement-based products. The microstructures of these products have been characterized in the fresh state, both normally cured and autoclaved, as well as after natural weathering in Switzerland and the Republic of South Africa. Characterization techniques include electron microscopy, used in both scanning and transmission modes, analytical electron microscopy, and pore structure analysis by mercury intrusion. Differences between cure regimes and exposure conditions are described. The change in the microstructure for both composites were intricate because of the non-isotropic nature of the products. Characterization of typical ageing development phases of the matrix was found to be very complex, although these extensive microstructural changes do not necessarily indicate that the performance of the material is adversely affected.

Keywords: Fibre–cement composites, durability, asbestos substitutes, microstructure, fibre-matrix interface, electron microscopy, pore structure, ageing, cracking (fracturing), composite materials.

INTRODUCTION

The durability of fibre reinforced cement composites can be documented for conventional asbestos cement products on the basis of experience. As some of the most important durability criteria are frost resistance, water-tightness, etc., priority is directed towards making the product 'functionable in service'. As formulations change, particularly in respect of fibre content and type, experience is no longer available for guidance. Short-term and accelerated testing can be used, but they present problems of interpretation. Mechanical properties can be determined as a function of time, but the basis of extrapolation is uncertain because the underlying mechanisms which give rise to property changes have, in most cases, not been clearly identified. The scientific validity of accelerated testing, particularly with respect to higher temperatures is also uncertain; cement-based material may enter a different physico-chemical regime at higher temperatures which may not be approached, even at very long ages, at more normal temperatures.

The cement-based composite material studied here consists of the matrix and reinforcing fibres. The matrix is composed of unhydrated cement clinker, hydrated cement products, quartz, non-reactive fillers and additives, and pores. The matrix interacts with fibre at the fibre–matrix interface where the so-called interfacial bond is formed. By its very nature the composite is anisotropic, and the concept of homogeneity in cement must be treated differently from the same concept, applied to other materials. The composite is very much 'alive' and during natural weathering changes such as continued hydration and carbonation continue. In fact even in Aspdin cement, some 140 years old, anhydrous clinker phases

Cement & Concrete Composites 0958-9465/91/$3.50

have been found to persist. It is, however, important to study the mechanisms of ageing in cement composites with particular relevance to their performance in service. The aim of this paper is to characterize

(i) changes in the mineralogy and microstructure of the matrix occurring with time,
(ii) the condition of the matrix–fibre interface, including bond development and ageing effects,
(iii) microstructural evidence for loss of ductility, reaction of cement phases and other characteristic features of fibre–cement interactions occurring during ageing of the composite.

These aspects have been closely examined for naturally-aged composites and compared directly with their non-aged equivalents. The products investigated include both normal and autoclaved asbestos-free fibre–cement products. This study forms part of an extensive durability programme in which many other aspects such as durability of the fibres in the composite have been addressed.[1–6]

EXPERIMENTAL PROGRAMME

Identification and product history

Samples of fibre reinforced cement products, typically 4–10 mm thick, were investigated. These were manufactured from the production lines in Switzerland and the Republic of South Africa, both processes using Hatschek machines. The products produced in Switzerland contained limestone as a filler, cement, amorphous silica and a mixture of synthetic (PVA) and cellulose fibres. These were moist cured at or near ambient temperatures and shall be referred to as normal cured synthetic–cellulose fibre products (Group A). The products produced in the Republic of South Africa contained cement, ground silica sand and cellulose fibres (*Pinus radiata*). The latter product composition was basically a 50:50 sand:cement mixture with the addition of 8% by weight of cellulosic fibres. These products were autoclaved, typicaly for 10 h at 10 bars, and shall be referred to as autoclaved cellulose fibre products (Group B). The products investigated were exposed to natural weathering. The microstructure of the matrix and interfacial bond were studied and compared with their unaged equivalent. The products from Group A and Group B were exposed to 5 years natural weathering in Switzerland (Niederurnen) and 4 years natural weathering in the Republic of South Africa (Johannesburg) respectively. These products fulfilled all the necessary service functions during the test duration. The products were removed from service in order to investigate their mechanical property development with age and at the same time study the ageing mechanism at a microscopic level.

Electron microscopy

Thin sections of the composites were produced by two methods for examination by electron microscopy.

Sectioning with a diamond knife

Samples of products, approximately 3 mm × 1 mm × 1 mm, unique in dimensions for orientation purposes, were embedded in resin and sectioned parallel to the plane of the fibres.

Sections of around 200 μm thickness were obtained from Group B products and examined by transmission electron microscopy. Products from Group A proved to be too hard for sectioning in this way, due to the presence of occasional silica grains (presumably from impurity in the limestone used).

Atom milling

Petrological thin sections, parallel to the plane of the fibres, were produced from each composite. These were subsequently atom milled for electron microscopy. The atom milling process can take several days for each sample. Efforts with this technique have concentrated on Group A composites. Since the atom milled sections used here are somewhat thicker than those sectioned using a diamond knife, they were examined in the electron microscope using the scanning transmission (STEM) mode.

Mercury intrusion porosity measurements

This technique involves the intrusion of a non-wetting, non-reactive liquid such as mercury into a porous material. Intrusion of the sample pores takes place under isostatically increasing pressure and the pore size intruded is inversely related to the pressure. This inverse relationship is expressed by the Washburn equation

$$D = \frac{-4\gamma \cos\theta}{P}$$

which is a capillary law governing liquid penetration into small pores where D is pore diameter, P

is pressure, γ is surface tension and $\cos\theta$ is the contact angle. The values used were $\gamma = 484$ dynes cm^{-1} and $\theta = 130°$.

RESULTS

Synthetic/cellulose fibre products (Group A)

Non-aged

The atom milled cross-section using the STEM mode is shown in Fig. 1. Two types of fibre are evident in Fig. 1 and there is a greater tendency of the synthetic fibre to orientate normal to the section, relative to cellulose. The synthetic polymer fibres (PVA) are nearly round in cross-section, whereas the cellulosic fibres are irregular. The polymer material is preserved in the section, but owing to its transparency, does not reproduce well in black-and-white photographs of the relatively homogeneous PVA fibre; the internal structure of the cellulosic fibre is better revealed. Contact between fibres and matrix and between individual particles within the matrix is generally good. When a chemical image for silicon (Si) is obtained quartz particles stand out clearly and can be distinguished from limestone particles. One region of Si penetration into the fibre is noticeable. The complementary calcium (Ca) and sulphur (S) images obtained by analytical microscopy (not shown) show that considerable Ca has impregnated the walls of the cellulose fibres, and some penetration into the fibre itself has begun. The corresponding map for S shows that it is also one of the more mobile constituents, filling the wall and penetrating the interior at isolated spots sympathetically with Ca. This points to a calcium sulphate phase, e.g. gypsum, as an important lumen-filling material.

Using the scanning electron microscope a representative selection of micrographs (Figs 2 and 3) are given. These are complementary to the transmission micrograph given in Fig. 1.

Figure 2 shows a wealth of microstructural detail. The cement matrix comprises irregularly shaped particles of various dimensions, cellulose and synthetic fibres, voids and areas of low density cement paste. Numerous clinker particles (C) are identified; cellulose fibres (F) and synthetic fibres (P) are prominent. The scanning

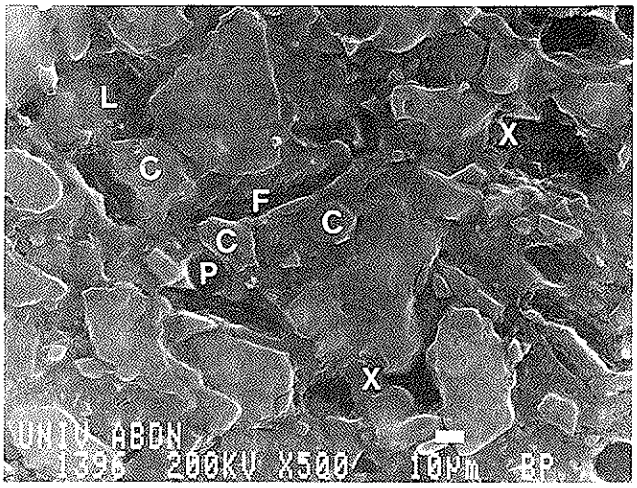

Fig. 2. Scanning electron micrograph of the non-aged product. C — clinker particles, F — cellulose fibres, P — synthetic fibres, and X — cement–fibre boundaries.

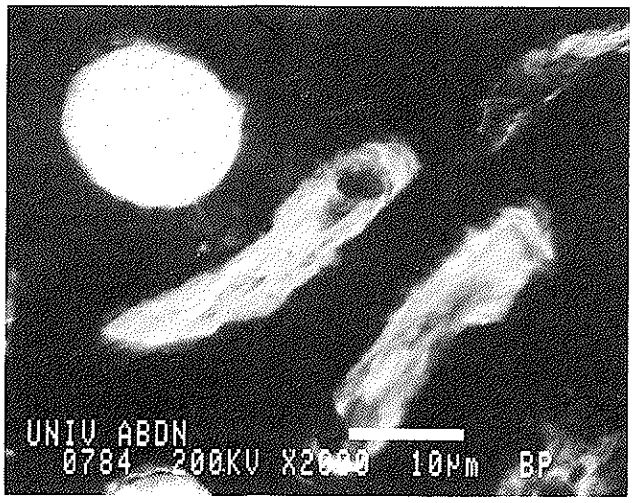

Fig. 1. Atom milled cross section of non-aged cement board containing both synthetic fibre (round cross-section) and cellulose.

Fig. 3. Scanning electron micrograph of non-aged product showing cracking. The arrow indicates microcracking confined to the cement matrix.

image confirms that the cellulose fibre lumens are mainly unfilled and shows that generally excellent physical contact is maintained between fibre and cement matrix.

It appears that the synthetic fibres generally lie at right angles to the section whilst the cellulose fibres display a lesser degree of orientation.

The area shown in Fig. 3 is an example of the interaction between cellulose fibres and microcracks. Two types of microcracking are seen; coarse microcracks, which tend to run through the matrix as well as a long cement–fibre boundaries (X) (although not suggesting weakening at this interface) and much finer microcracks. The latter are largely confined to within the cement matrix (arrowed). Some may be elongated voids, i.e. cross-sections of microcracks lying perpendicular to the section.

Natural weathered, 5 years

The transmission image, Fig. 4, with the assistance of elemental maps, (not shown) reveal the presence of hydration products (H) with high Si, Ca and S, the clinker (C) as having Si and Ca, and the limestone particles (L) with high Ca only.

The uncommon sharp-edged particles, one of which is arrowed (upper right), have high levels of aluminium (Al), moderate Ca and no Si. Their identity is uncertain, but they could be fragments of the alumina abrasive used in the initial thinning of the petrological section. The particles (X) containing Al, S, Ca and iron (Fe) suggest formation of a calcium monosulphate aluminate hydrate, designated AF_m phase, rather than an ettringite, AF_t type phase as the latter would, if present, show an enhanced sulphur signal at these regions.

Scanning electron micrographs complementing the transmission micrographs of Fig. 4 are given in Figs 5 and 6. Figure 5 shows substantial areas which, by their slightly granular microstructure appear to be thoroughly carbonated. Two types of microcracking are evident: coarse cracks at lower right and finer cracks (arrowed) or elongated pores within the cement matrix. The microcracks generally tend to run normal to the surface of the section and pockets of porosity (S) are associated with their path. The crack along the cellulose fibre

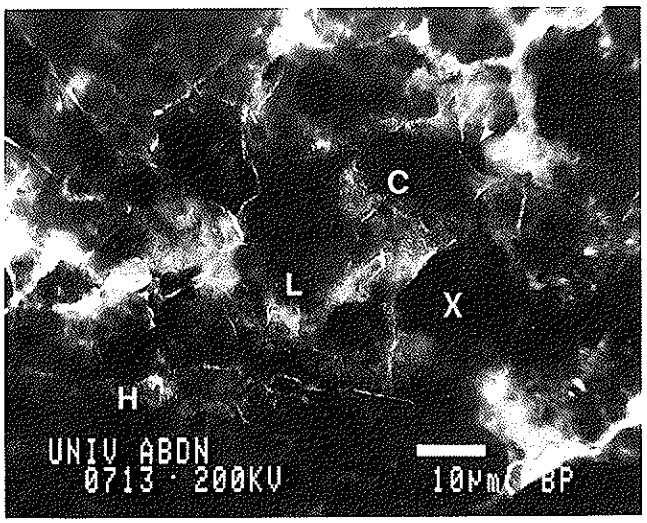

Fig. 4. Atom-milled cross sections of naturally-weathered, five-year-old product. C — clinker particles, H — hydration products, X — cement–fibre boundaries, and L — limestone particles.

Fig. 5. Scanning electron micrograph of naturally weathered, five-year-old material showing intensively carbonated matrix. F — cellulose fibres, and S — pocket of porosity.

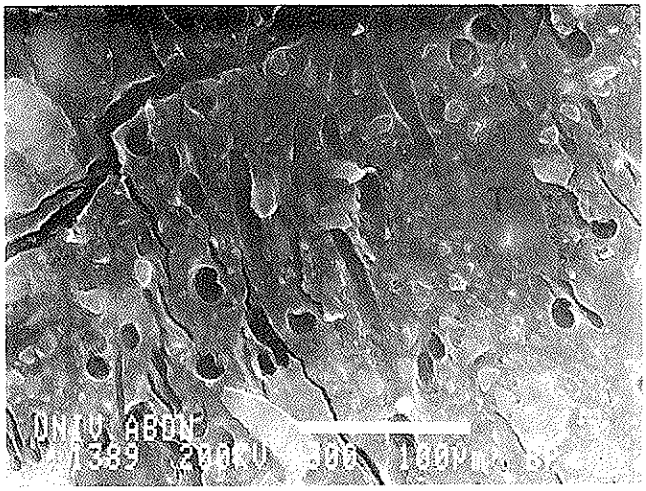

Fig. 6. Fibre-rich area of naturally-weathered five-year-old material. T — a relic of a large clinker grain which has undergone hydration and carbonation.

(F) is tentatively ascribed either to shrinkage of the material or, less likely, to transfer of material from the outer margin of the fibre into its lumen. Synthetic fibres lying at right angles to the section are observed (P); their orientation is quite characteristically different from those of the cellulose fibres. An area with dense clustering, particularly of synthetic fibres, is seen in Fig. 6. There is a slight suggestion in this micrograph that clustering of fibres may determine crack direction but a wide range of fibre orientations are evident in this area. It is noted that where fibres lying parallel to the plane of section have been etched away by atom milling, the remaining imprint displays a degree of roughness on the walls. This may be the remains of fibre material, rather than an indication of porosity in the adjacent matrix, so it is concluded that bonding generally remains satisfactory. Clinker particles are prominent in the cement matrix but some of the smaller grains may be calcium carbonate (arrowed). The smooth triangular area (T) is likely to be a relic of a large clinker grain which has undergone hydration and carbonation, and is now merging with the background matrix. During the course of carbonation, some solution–reprecipitation reactions are likely to occur and it is not surprising that occasional cracks are favourably located with respect to filling. Crack rehealing occurs commonly and is an important process whereby the material can maintain its integrity during weathering.

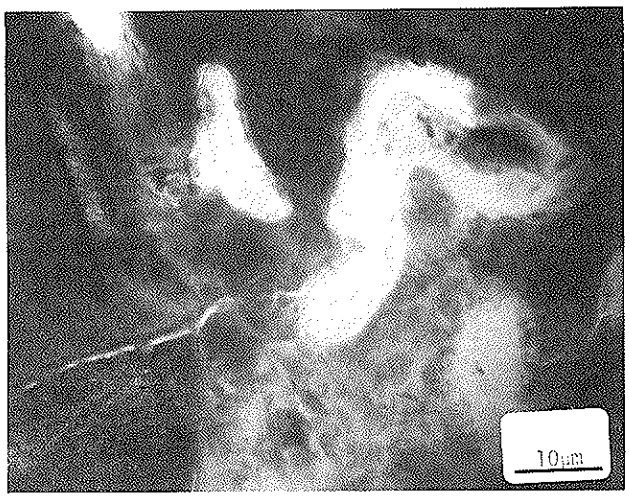

Fig. 7. Autoclaved fibre–cement fresh composite, showing the transmission image.

Autoclaved cellulose fibre products (Group B)

Non-aged

The *Pinus radiata* fibres (tracheids) used in this composite generally displayed a twisted or distorted appearance in the cement matrix, as shown in Fig. 7. Despite their irregular shape, the lumen appears to remain open, although largely devoid of solid mineral content. Chemical image mapping discloses that a thin layer of cement matrix covers the fibre, indicating generally good and continuous contact between fibre and cement. A quartz particle is evident at the upper right with a definite crack along its edge running towards the fibre. There is evidence of reaction product around the quartz particle; note the presence of a distinct rim along its edges. There appears to be two types of contact around fibres, (a) a rim close to the fibre and (b) cement paste, pressed against the fibre, exhibiting needle-shaped structures. The general matrix displays several enigmatic features in the form of needle-shaped crystals and filament-like structures. These needle-shaped crystals were examined by selected area electron diffraction and proved to be tobermorite. The presence of abundant tobermorite in this composite was also confirmed by X-ray diffraction studies. It is thought that the needle structures may in part consist of plate-like tobermorite crystals viewed laterally, giving the impression of needles. The interpretation of these textures is that the autoclaving treatment has produced variable degrees of conversion of low-temperature hydrate and silica to tobermorite and, moreover that a range of crystallite sizes and perfection occur.

A scanning micrograph of this area reveals the microstructure detail (Fig. 8a): the cement matrix comprises various structural characteristics including needle-shaped crystals, smooth plates, distinct particles and amorphous areas intermingling with each other to produce a very heterogeneous appearance. The microcrack along the quartz particle boundary is of particular interest and is shown at higher magnification in Fig. 8b. The fringe around the particle, seen in transmission (TEM), is confirmed in scanning mode (SEM) as a layer of needle-like crystals. Spot X-ray microanalysis performed at A, B, C and D give Ca:Si ratios of 1:36, 5:6, 1:1 and 5:3 respectively. The bundle, B, of needle-shaped crystals is therefore tobermorite and the crack follows closely the boundary between this tobermorite rim and the unreacted silica core. Although this may indicate the line of least resistance, suggesting that the weakest bond is between the unreacted particle

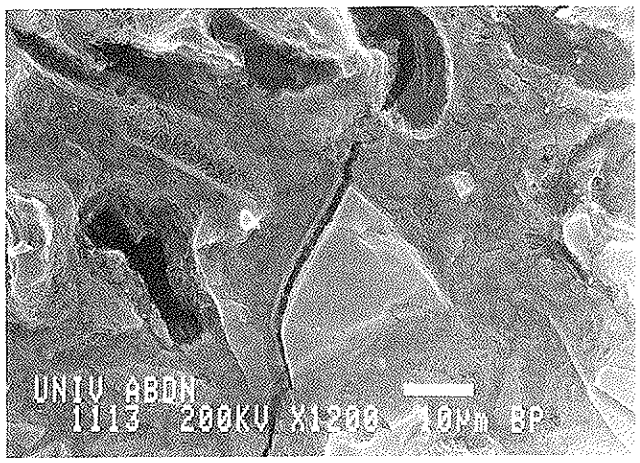

(a)

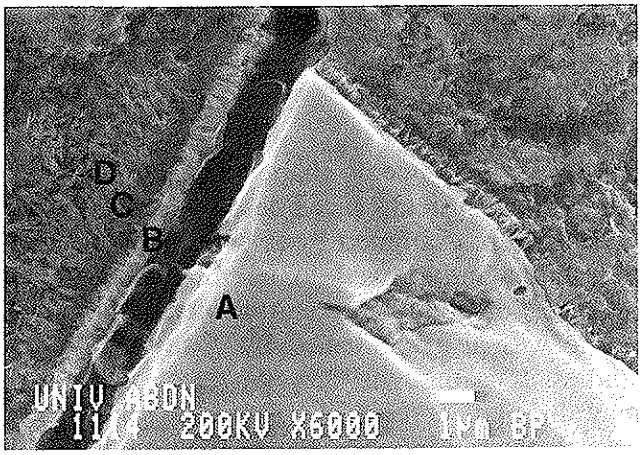

(b)

Fig. 8. Scanning electron micrographs of autoclaved fibre–cement fresh composite. (a) Shows the overall texture and (b) the appearance of microcracking adjacent to an unreacted quartz grain.

and the matrix, it should be noted that the crack void does appear to be bridged by a gel-like substance. Another crack is seen at the top right of the field and is again being stopped by a fibre. The hole in the other fibre is due to the atom milling process which causes the fibre to thin more rapidly than the surrounding matrix.

The general impression gained from the TEM and SEM images is that the silica particles strongly influence the microstructure and composition of the surrounding matrix, indicating that one of the primary aims of the autoclaving treatment, namely development of a mixed C—S—H and tobermorite matrix, has been achieved.

Naturally weathered materials

In essence the microstructure of these aged products is much changed as a consequence of environmental exposure. Of course certain features, such as the distribution of quartz grains and fibres persist unchanged. Therefore, the microstructural investigation has concentrated on changes with respect to fresh material. The fibre lumens become filled with calcium-containing material and, as a result of tobermorite in the matrix being destroyed by carbonation, the matrix texture becomes more crystalline.

Figure 9 shows a fibre sharply folded back against itself presumably as a result of fabrication. However, this has not prevented penetration of calcium into the lumen. The presence of calcium, but not silicon, within the lumen is shown on chemical X-ray maps. The lumen contents are likely to be $CaCO_3$, but sulphur is also present, suggesting that part of the calcium is present as calcium sulphate. The matrix also displays several enigmatic features; the filamentous material at the top right and the area of clumped material, which may be underlying the fibre, should be noted. Silicate particles are predominant, but quartz reaction rims, as observed in non-aged composites, are seldom detected in aged samples.

Microcracking of the cement matrix is more extensive in aged products and Fig. 10 is typical. Some cracks could be described as voids whilst others are hairline, and vary in length. Cracks can be discovered in practically any field of view in the aged material. The impression given is that this material is inherently microcracked to a much greater extent than fresh product. While some crack rehealing may have occurred, it has been at an insufficiently rapid rate to present an overall increase in microcrack density.

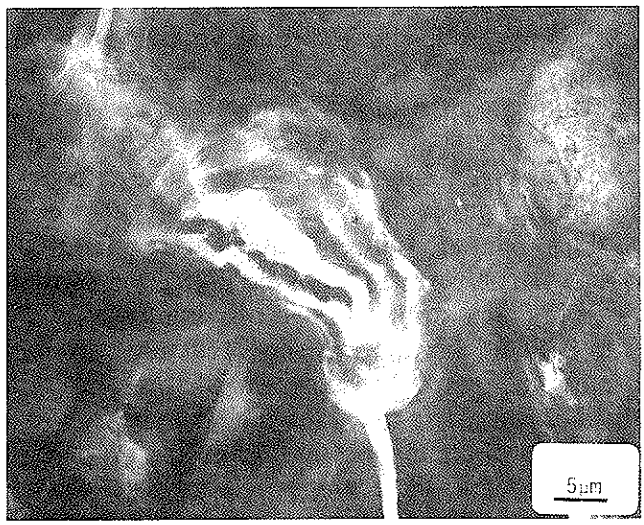

Fig. 9. Naturally-aged, three-year-old autoclaved material.

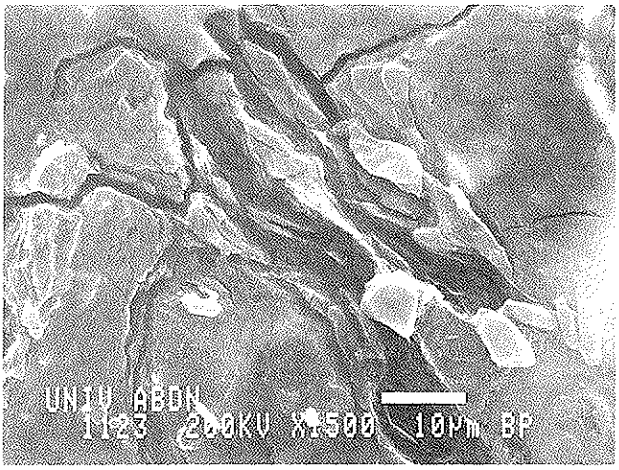

Fig. 10. Scanning electron micrograph of the naturally aged, three-year-old autoclaved material showing the extensive microcrack network.

The background matrix generally presents a very different image to that seen in non-aged composites. The absence of needle-shaped crystals is immediately apparent; thus the matrix presents a more compact and uniform texture interspersed with relics of unreacted silica particles. The crack network again appears to be an intrinsic feature of the aged material. In Fig. 11a, the large particle (top, centre) near the fibre is a quartz grain, but Ca is predominant in all other areas. The paler gel-like substance above it comprises mainly Ca and Fe; a fibre enters the field from the right. In Fig. 11b, the fibre is predominant. It should be noted that even in regions of high fibre density, cracking does not pass through the fibre. Areas formerly comprising tobermorite needles and silica particles can be identified on close inspection.

Mechanical property evolution of the composite

In this section only a brief description of the evolution of the mechanical properties of the composite is given, as these trends have been reported elsewhere.[5] The results presented in Table 1 represent the absolute values obtained from a simple three-point flexural test. In essence, the aged composites reveal an increase in flexural strength and E-modulus. However, no relevance is attached to the absolute values and only the trend in mechanical property development should be treated as significant.

It should be borne in mind that the microscopical results reveal an increase in microcracking with age; however, this does not appear to influence the strength of the product adversely and

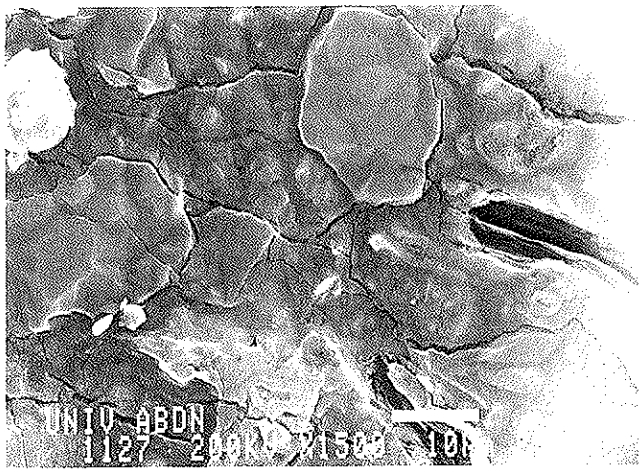

(a)

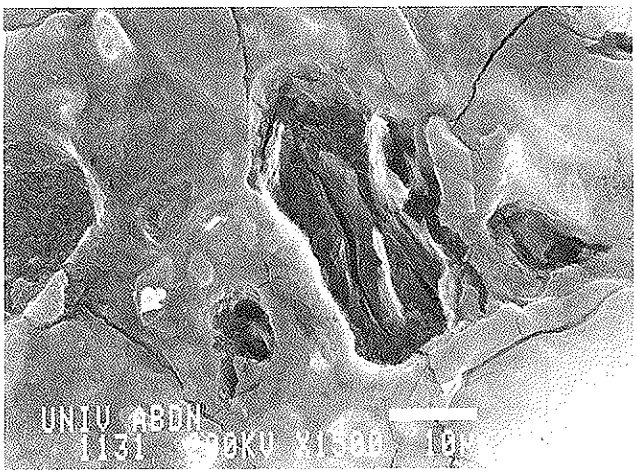

(b)

Fig. 11. (a) and (b) electron micrographs of the naturally aged three-year-old, autoclaved material. See text for a description of the principal features.

it may be considered that the increase in microcracking with age is overridden by other matrix or fibre–matrix reactions. In fact, microcracking may be considered together with the larger irregularly-shaped pores and low density zones as general sources of mechanical weakness, with the result that during the course of weathering, a redistribution of the total void space occurs between larger pores, low density zones and microcracks with the result that the overall mechanical performance remains substantially unchanged.

Porosity measurements

Synthetic–cellulose fibre products (Group A)

Tests were performed on non-aged and naturally aged products; the results are given in Figs 12–15. Figures 12 and 13 show incremental volume plots (increment volume plotted against pore diameter) for the non-aged and aged respectively.

Table 1. Mechanical properties of normal cured synthetic–cellulose fibre (Group A) and autoclaved cellulose fibre (Group B) products

Products	*Flexural strength (MPa)*	*E-modulus (GPa)*	*Limit of proportionality (MPa)*
Group A			
Non-aged	28·6 ± 2·1	16·0 ± 1·6	26·2 ± 1·1
Natural weathered 5Y	31·9 ± 0·9	18·5 ± 1·3	28·1 ± 0·6
Group B			
Non-aged	17·6 ± 0·3	7·6 ± 0·3	16·1 ± 0·5
Natural weathered 4Y	27·2 ± 0·6	18·6 ± 0·3	25·9 ± 0·9

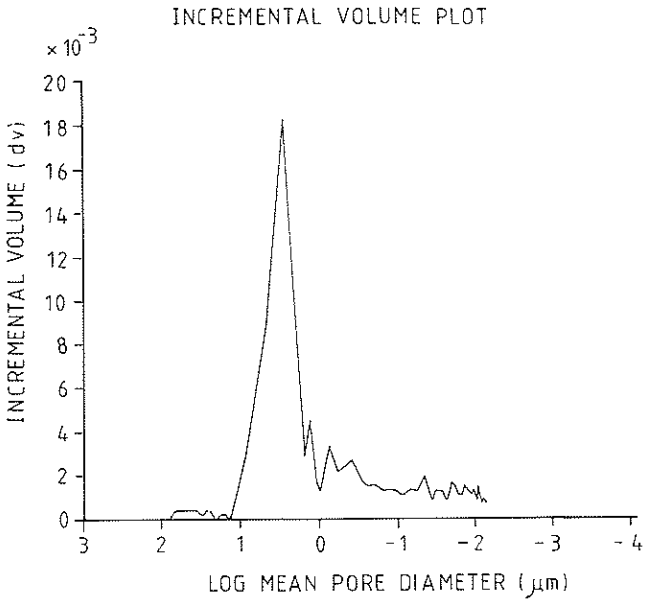

Fig. 12. Incremental Mercury Intrusion Porosity (MIP) scan of fresh product.

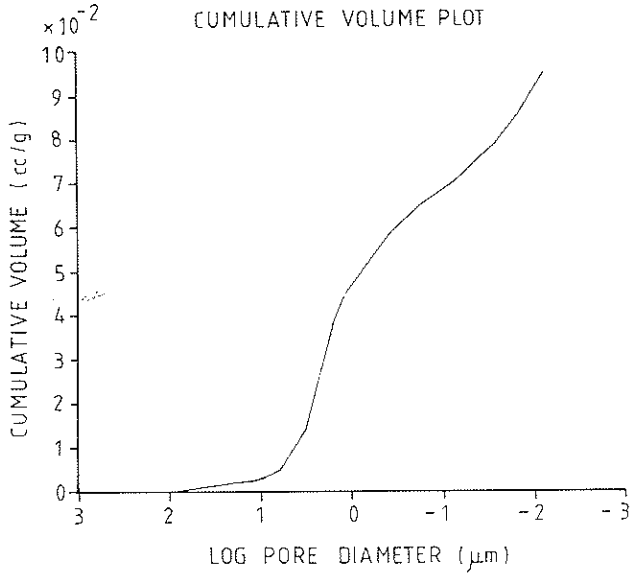

Fig. 14. Cumulative MIP scan of fresh product complimentary to Fig. 12.

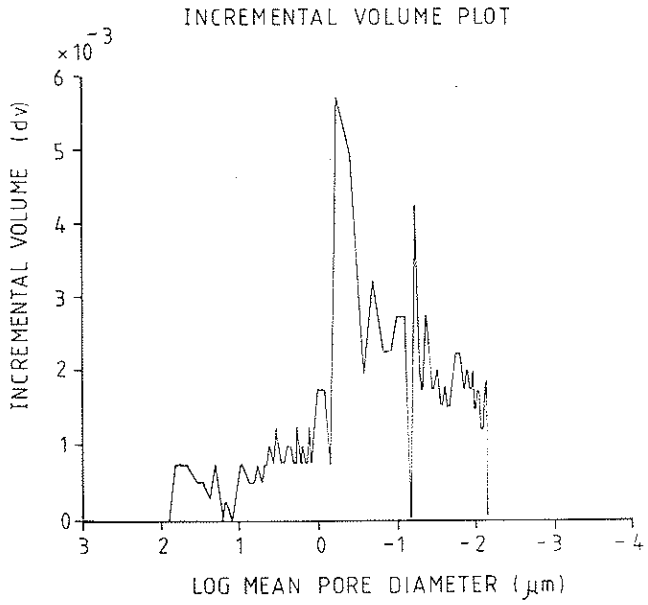

Fig. 13. Incremental Mercury Intrusion Porosity (MIP) scan of naturally-aged product.

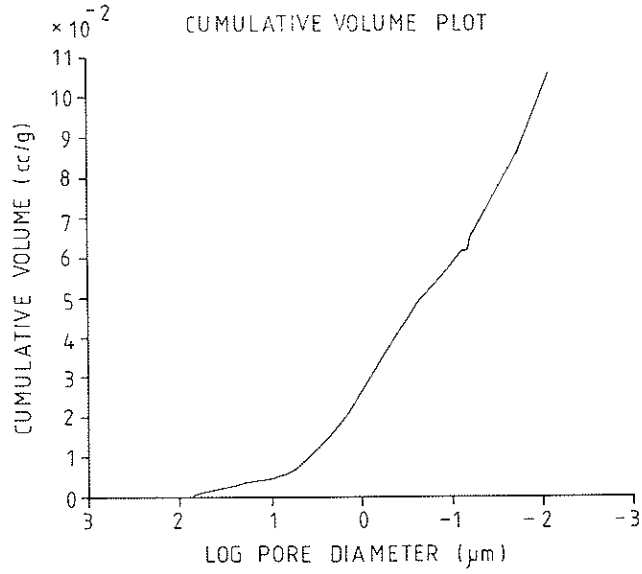

Fig. 15. Cumulative MIP scan of naturally-aged product complimentary to Fig. 13.

It should be noted that the vertical scales differ slightly in magnitude between graphs. The pore diameter decreases from left to right along the axis and represents analysis from low to high pressures respectively.

The cumulative volume plots for the non-aged and aged are shown in Figs 14 and 15 respectively, and indicate that there has been significant redistribution of pores. These aspects will be discussed in detail in the next section.

Autoclaved products (Group B)

The results for non-aged and aged products are given in Figs 16 and 17. These show incremental volume plots (incremental volume plotted against pore diameter) for non-aged and aged materials respectively (note that the vertical scales are of different magnitude in each graph). The pore diameter decreases from left to right along the axis as the analysis sweeps from low to high pressures respectively. The plots are reasonably similar with the exception of the large peak at mean pore diameters $> 4\ \mu m$, (Fig. 16).

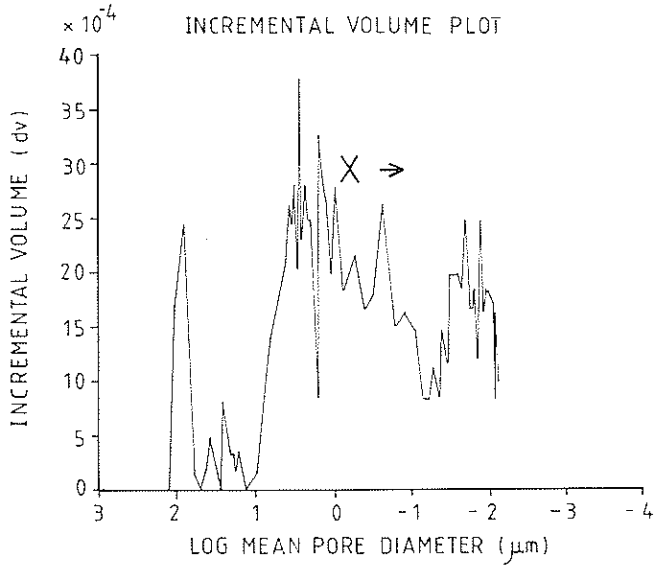

Fig. 16. Incremental MIP scan for autoclaved fresh product.

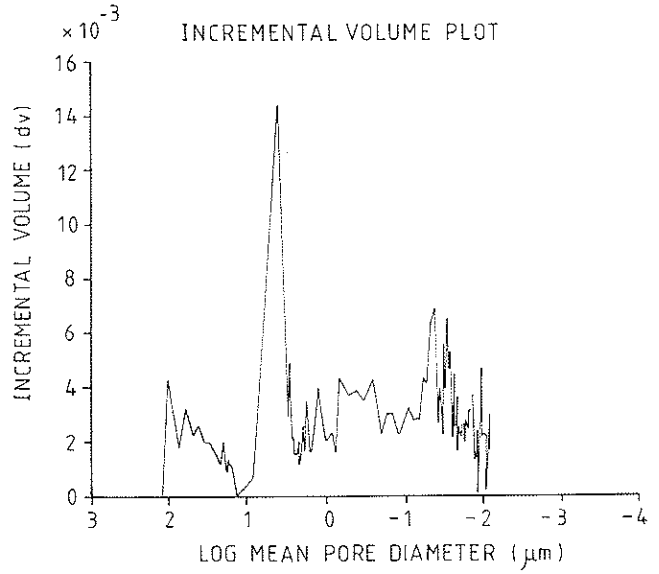

Fig. 17. Incremental MIP scan for autoclaved, naturally-weathered product complimentary to Fig. 16.

DISCUSSION

Examinations of all the products presented in this paper do not enable the authors to point unequivocally to a single factor which is responsible for the changes in properties occurring during natural ageing. The changes which occur are complex, and undoubtedly cumulative in their effect on properties. Moreover, certain parameters of the manufacturing process are essentially fixed, at least while present processing methods continue in use, and process constraints condition to a significant extent the properties of the product. Thus, certain microstructural features persist throughout the curing and ageing of the materials. These can be interpreted in terms of their process history — autoclaved or non-autoclaved — and subsequent exposure.

Normal cured synthetic–cellulose fibre cement products

The first aspect is the nature of the hydration process occurring in these materials. Normally, cements are mixed with water at water:cement ratios between, say, 0·35 and 0·55. Once mixed, the blend is placed and allowed to set and harden undisturbed; initial set is retarded by the use of sparingly soluble sulphate, e.g. gypsum. This is also true of other sheet-like cement products, such as roof tiles made by extrusion. However, in the Hatschek process, setting occurs somewhat differently. The cement is initially mixed to a very much higher water:cement ratio, sufficient to give a fluid slurry, and the resulting slurry is then used to build up a sheet material which is dewatered and thickened on the drum. The length of time which elapses between adding fresh cement to the bath and its eventual removal on the process drum (whereafter it quickly takes the form of sheet) is not constant, but is largely statistical and hence variable from one cement grain to another. Thus some grains may remain in the slurry for a long time and undergo a significant amount of

prehydration resulting in formation of a coating of low-density hydrate. In a normal cement blend, this does not occur as the set is well regulated by the quantity of retarder present, which would be sufficient to present significant hydration occurring for some fixed period, typically several hours. However, equal retardation is unlikely to occur for all grains in the Hatschek process; not only is the amount of water abnormally large by normal standards (which upsets the retarding action), but hydration of cement is also autocatalytic; even a few hydrating grains which may have gone past their induction period absorb sulphate ions from solution, allowing the remaining grains to hydrate more rapidly. Thus the excess of water present in the Hatschek process may upset the action of the retarder, which is calculated to perform at much lower water:solid ratios. The occurrence of active hydration prior to forming is supported by the evident self-heating which occurs: fresh sheet is already perceptibly warm even when still on the roller drums. Hydration product formed at the slurry stage has a low density and is unlikely to form strong bonds between grains during subsequent forming, unless mechanically compacted. Suction forming roller compaction and stack pressing are unlikely to give sufficient consolidation to densify the soft gel significantly.

Loss in ductility during ageing is viewed as arising from two causes. Firstly, the fibre content is subject to change. Microscopically, synthetic polymer fibres persist unchanged, but the lumen of cellulosic fibres gradually become filled, at least in part, with cement hydration products. As carbonation of the matrix occurs the fibre fillings also carbonate and more sulphate migrates. As a consequence, the fibres lose flexibility and become more brittle. Cement gel is porous, and hence flawed and intrinsically weak, but it is relatively continuous in the sense that it contains no micrometer-sized intercrystalline boundaries, other than those formed at its margins with $Ca(OH)_2$ grains: the latter are, in any event, even absent in autoclaved product. Secondly, as carbonation progresses, new intercrystalline boundaries develop within the space formerly occupied by gel as $CaCO_3$ (calcite) crystallizes. It is suggested that the slight flexibility of the cement paste gel which enables it to absorb energy gel prior to fracture now gives way to another stress failure mode involving grain boundary sliding and interaction with the extensive microcrack network. This, in conjunction with the relatively low local density of the hydration products, as well as migration of material during weathering and carbonation, enhances the tendency towards a brittle failure mode. Considering the porosity of the product and its development with age, the significance of the graphs presented can be analyzed by examining the pore size distribution in different ranges. The large peak, around 3–5 μm pore diameter, is an important characteristic of fresh material (Fig. 14). Whilst this range corresponds to the lumen diameter range of the cellulose fibre, this alone cannot account for the large intrinsic volume in this range because only the comparatively few exposed lumens of broken fibres are accessible to mercury. Moreover, the lumens of aged material are already partly filled. With the exception of the broken fibres, filling of any remaining void in the lumen must occur through the pores on the fibre walls. As these transverse pores are extremely fine, the effect, if any, is likely to add to the total porosity only within the finest pore sizes accessible to mercury. Thus the 3–5 μm peak has to be ascribed to other origins and is believed to arise mainly from filling of microcracks and spaces in outer hydrate material.

After 3 years natural ageing the 3–5 μm peak has disappeared (Fig. 13), the incremental volume having decreased from a maximum of 18×10^{-3} to a background level of 1×10^{-3} cm^3 g^{-1}. This suggests that these larger voids have become filled, or at least blocked, by hydration and carbonation products in the course of ageing; it is also known that some lumen filling has occurred. The incremental volume in the 0·1–1·0 μm range has risen slightly over three years, and can be related to a decrease in the mean diameter of larger pores as a result of partial filling and pore entry blocking. These factors, together with continued hydration and carbonation, work cooperatively with the result that the peak in pore size distribution is shifted into the ~0·5 μm diameter pore regime.

These observations are confirmed by electron microscopy which shows a distinct change in texture between fresh and aged material. The cumulative volume plots also suggest that there is not a great deal of difference in total porosity, but that significant differences occur arising from changes in pore shape and pore size distribution. The total porosity is however slightly greater in the 3 year aged material, especially in the 10–100 μm pore diameter range, relative to fresh material. This shows as the large blip in the incremental volume plot (Fig. 13). This feature is believed to be related to the cracking observed by electron microscopy in composite aged for 3

years, and confirms that although some cracking may be extrinsic — caused by specimen preparation for microscopy — the greater proportion of the cracking is intrinsic, and is considered to be the result of chemical and microstructural stresses occurring as a consequence of the weathering process.

Superimposition of the graphs in Figs 14 and 15 show that the cumulative porosity in the smaller pore diameter region, 0·1–1·0 μm, is less after 3 years ageing. This represents the results of the continuing processes of hydration and carbonation and crack healing. However, in common with other cement materials, both composites, whether fresh or aged, are relatively porous.

It would appear that upon ageing, development of the matrix and interfacial (fibre–matrix) bond is too complex to correlate pore size and pore size distribution alone with evolution of the mechanical properties, but that certain well-defined trends do occur.

Autoclaved cellulose fibre–cement products

Autoclaving substantially changes the texture, microstructure and mineralogy of the material with respect to the normally-cured product. Nevertheless, many textural features inherited from the original fabrication and short normal cure still persist and many of the remarks concerning the effect of processing on properties of normally cured materials are also true of autoclaved products. For example, despite the intensity of the autoclaving, clinker still persists, indicating that insufficient water was available to complete the hydration process. Moreover, the conversion of C—S—H gel to tobermorite is patchy; some areas are well converted, while others are almost unconverted or only partly converted. The low degree of conversion to tobermorite, as well as the presence of unreactive clinker, also implies that much silica flour, which could potentially be consumed, remains unreacted. The natural organic 'fibres' in the autoclaved material have a less favourable aspect ratio than those of the normally cured product and, it is suggested, the latter are rather marginal in the morphological sense with respect to their classification as 'fibres'. The incomplete or arrested reactions occurring in the autoclaved material make it difficult to assess its potential for durability, especially as the extent to which reaction has progressed is so variable from one sample to another, as well as at different points within any one sample.

The overall pore volume of the fresh material is greater than in the composites aged 4 years because, as ageing proceeds, many voids gradually fill with hydration and carbonation products. Thus pores with small diameters, <1 μm, are unlikely to represent the same pores as in fresh material after 4 years exposure: owing to migration of material, their locus changes. The composites aged for 4 years displayed extensive microcracking by electron microscopy. These cracks varied in width but did normally exceed 0·5 μm. It may, therefore, be proposed that the incremental volume present for pore diameters $<0{\cdot}5$ μm, i.e. like the pore shown to the right of point X in Fig. 16, represent the cracking features identified in the aged samples. The two curves shown in the cumulative volume plots. Figures 16 and 17, are significantly similar, which suggests that some features of the original microstructure are preserved.

CONCLUSIONS

(i) It is apparent that the composites examined comprise non-homogeneous mixtures, having an uneven distribution of particulate components and fibres; some regions are indeed devoid of fibres. This inhomogeneity, believed to be related to processing, creates domains of differing microstructure and mechanical properties.

(ii) Non-aged, normal cured synthetic fibre composites contain much unhydrated cement clinker but a good bond forms between fibres and matrix. Nevertheless, the fresh paste hydrate material is rather porous, on account of the generally low degree of hydration: spaces between clinker grains and aggregate particles tend to be filled with rather low density cement paste.

(iii) The degree of hydration in the normally cured synthetic fibre product is enhanced by natural weathering. The matrix begins to show evidence of more recrystallization; iron, expelled from silica gel and calcite, segregates into small regions, perhaps containing one or more iron hydroxides. Nevertheless, many of the larger-scale microstructural features broadly resemble those of fresh material, and even at 3 years, some clinker still persists.

(iv) The non-aged autoclaved products contain a more complex microstructure than the normal cured products. Quartz grains participate in the

reaction during autoclaving, and are surrounded by a duplex layer structure, characterized by an inner zone consisting mainly of tobermorite needles and plates, and an outer zone of relatively dense hydration product. These have a mean Ca:Si ratio close to 1·0. This is believed to consist of a mixture of tobermorite and C—S—H; electron diffraction and X-ray diffraction supports the view. The contact between quartz grains and inner tobermorite products appears to mark a zone of mechanical weakness. This zone is particularly conspicuous around the larger quartz grains. Pore structures, presumably inherited from the original processing, are evident, but autoclaving has partly filled these pores with needles (tobermorite) and foils (C—S—H). $Ca(OH)_2$ is essentially absent.

(v) In the course of natural ageing of autoclaved products, much mineralogical and microstructural change occurs. Tobermorite and C—S—H become carbonated. Microcracking becomes much more extensive although crack healing also occurs to a limited extent. The lumen of fibres becomes filled, at least partially by Ca, S, presumably as calcium carbonate and sulphate.

(vi) The cement matrix of both products examined is very porous. Ageing changes the size and shape of the pores, including voids, but the total porosity decreases only slightly. In conjunction with electron microscopy, many of the 'pores' — especially those in the larger size range — have dimensions and shapes which are best described as cracks. Fibre reinforcement and crack healing are partially successful in containing crack growth and mitigating its effect on mechanical properties.

ACKNOWLEDGEMENT

The authors thank Dr E. Lachowski for his assistance with the interpretation of the electron micrographs and preparation of the photographic prints.

REFERENCES

1. Studinka, J. B., Asbestos substitution in the fibre-cement industry. *Inter. J. Cement Composites and Lightweight Concrete*, **11** (2) (1989) 73–88.
2. Akers, S. A. S., Studinka, J. B., Meier, P., Dobb, M. G., Johnson, D. J. & Hikasa, J., Long-term durability of PVA reinforcing fibres in a cement matrix. *Inter. J. Cement Composites and Lightweight Concrete*, **11** (2) (1989) 79–92.
3. Akers, S. A. S. and Studinka, J. B., Ageing behaviour of cellulose fibre cement composites in natural weathering and accelerated tests. *Inter. J. Cement Composites and Lightweight Concrete*, **11** (2) (1989) 93–8.
4. Bentur, A. & Akers, S. A. S., The microstructure and ageing of cellulose fibre reinforced autoclaved cement composites. *Inter. J. Cement Composites and Lightweight Concrete*, **11** (2) (1989) 99–110.
5. Bentur, A. & Akers, S. A. S., The microstructure and ageing of cellulose fibre reinforced autoclaved cement composites. *Inter. J. Cement Composites and Lightweight Concrete*, **11** (2) (1989) 111–16.
6. Akers, S. A. S., Crawford, D., Schultes, K. & Gerneka, D. A., Micromechanical studies of fresh and weathered fibre cement composites, Parts I and II. *Inter. J. Cement Composites and Lightweight Concrete*, **11** (2) (1989) 117–32.